

# Effect of the Nature of the Additives of Metal Cations (Sr, Ba, and La) on the Properties of Co–Mo Hydrodesulfurization Catalysts

E. V. Korneeva, A. S. Ivanova, G. A. Bukhtiyarova, P. V. Aleksandrov,  
V. I. Zaikovskii, I. P. Prosvirin, and A. S. Noskov

Boreskov Institute of Catalysis, Siberian Branch, Russian Academy of Sciences, Novosibirsk, 630090 Russia

e-mail: kulko@catalysis.nsk.su

Received July 5, 2010

**Abstract**—The effect of the nature of the support modified with the ions of alkaline earth and rare earth elements (Sr, Ba, and La) on the properties of Co–Mo catalysts for the hydrodesulfurization of dibenzothiophene (DBT), 4-methyldibenzothiophene (4-MDBT), and 4,6-dimethyldibenzothiophene (4,6-DMDBT) was studied using a set of physicochemical and catalytic techniques. It was found that the introduction of modifying additives decreased the surface concentration of Lewis acid sites (LASs) and increased the concentration of basic sites (BSs) in aluminum-containing supports; these changes were more significant upon modification with lanthanum and strontium. The modification affected the distribution and degree of dispersion of Co–Mo–S sulfide packets. It was found that the rate constants of DBT and 4-MDBT conversion increased with decreasing total surface concentration of both LASs and BSs on the support. The highest rate constant of 4,6-DMDBT conversion was reached at an optimum concentration of weak Lewis sites on Co–Mo catalysts, whose support was modified with strontium or barium.

**DOI:** 10.1134/S0023158411030128

## INTRODUCTION

Numerous sources of environmental pollution include insufficiently purified fuels containing sulfur and other impurities. Therefore, hydrofining is a basic large-scale process of petroleum refining, and its role increases because of stricter requirements imposed on the sulfur contents of gasoline and diesel fuel [1, 2].

Sulfide Co(Ni)–Mo catalysts supported on  $\text{Al}_2\text{O}_3$  are widely used in the hydrodesulfurization of fuels [3, 4]. The activity of the Co(Ni)–Mo catalysts depends on the degree of dispersion of the active constituent and its distribution on the support surface, as well as on the ease of sulfidation. These properties mainly depend on the nature of the support, primarily, on the degree of its interaction with the active constituent [5–7]. In addition to acid supports, such as  $\text{Al}_2\text{O}_3$ ,  $\text{SiO}_2$ – $\text{Al}_2\text{O}_3$ , and zeolites [4, 7–9], basic systems are of considerable interest, and the applicability of these systems as catalyst supports has been studied [10–12]. Such supports are interesting for the following two reasons: First, the acid–base interaction between acid  $\text{MoO}_3$  and a basic support in an oxide precursor of sulfide catalysts facilitates the high and stable degree of dispersion of a Mo-containing component. Second, the basic nature of the support inhibits coking, which intensely occurs on aluminum oxide catalysts [13].

In particular, Zdražil [14] demonstrated that the introduction of  $\text{MgO}$  into an aluminum oxide support facilitated the formation of short  $\text{MoS}_2$  packets and

increased the surface area of a boundary plane suitable for promoting with cobalt. According to Wu et al. [15], the addition of  $\text{MgO}$  effectively suppressed the formation of an inactive phase of  $\text{CoAl}_2\text{O}_4$  and prevented coke formation reactions. The activity of a catalyst in hydrodesulfurization can be considerably increased at a high  $\text{MgO}$  content of the support. Analogous results were obtained upon the modification of a support with  $\text{CaO}$  [10]: Mo and Ni–Mo catalysts supported on alumina modified with  $\text{CaO}$  exhibited higher performance characteristics in hydrodesulfurization and hydrogenation and a lower degree of deactivation due to coke deposition. This was due to structural differences between various Mo species formed on the surface of a modified support. The presence of  $\text{Ca}^{2+}$  ions inhibited the formation of  $\text{MoO}_3$  and  $\text{Al}_2(\text{MoO}_4)_3$  phases. It was found that the reason for the higher observed catalytic activity of the samples on the modified support was a higher degree of sulfidation. Thus, the Ni–Mo/Al–Ca sample exhibited higher catalytic activity before and after coke formation. In this sample, the degree of molybdenum reduction to  $\text{Mo}^{4+}$  (i.e., the ratio  $\text{Mo}^{4+}/(\text{Mo}^{5+} + \text{Mo}^{6+})$ ) was lower but the degree of sulfidation (the ratio  $\text{S}/\text{Mo}^{4+}$ ) was higher than those in the samples containing the unmodified support. It is well known that the electronegativity of the  $\text{La}^{3+}$ ,  $\text{Sr}^{2+}$ , and  $\text{Ba}^{2+}$  ions is lower than that of the  $\text{Mg}^{2+}$  ion. However, there are almost no published data on the influence of  $\text{La}_2\text{O}_3$ ,  $\text{SrO}$ , and  $\text{BaO}$  introduced

into aluminum oxide on the properties of the resulting Co–Mo hydrodesulfurization catalysts.

This work was devoted to a study of the effect of the nature and concentration of alkaline-earth and rare-earth oxides introduced into aluminum on the physicochemical and catalytic properties of Co–Mo catalysts for the hydrodesulfurization of fuels.

## EXPERIMENTAL

**Preparation of supports.** Aluminum hydroxides modified with alkaline-earth and rare-earth cations M (M = Sr, Ba, and La) were obtained by precipitation from the mixed solutions of the corresponding salts with a solution of ammonium bicarbonate ( $\text{NH}_4\text{HCO}_3$ ,  $\rho = 1.055\text{--}1.064 \text{ g/cm}^3$ ) at a constant pH  $\sim 7.0\text{--}7.2$  and a temperature of  $70^\circ\text{C}$  with the subsequent aging of the suspension for 3 h. Pure aluminum hydroxide was prepared in a similar way. The salts were  $\text{Al}(\text{NO}_3)_3 \cdot 9\text{H}_2\text{O}$ ,  $\text{La}(\text{NO}_3)_3 \cdot 6\text{H}_2\text{O}$ ,  $\text{Sr}(\text{NO}_3)_2$ , and  $\text{Ba}(\text{NO}_3)_2$ . After aging, the suspension was filtered and washed with distilled water. The precipitate was dried in air and then in a drying oven at  $120^\circ\text{C}$  for 16–18 h. Then, the samples were calcined at  $550^\circ\text{C}$  for 4 h in a flow of dried air. The supports were designated as AMn, where A is  $\text{Al}_2\text{O}_3$ , M = S, B, or L (S is  $\text{SrO}$ , B is  $\text{BaO}$ , and L is  $\text{La}_2\text{O}_3$ ), and  $n = 1$  or 5 mol %.

**Preparation of catalysts.** The catalysts were prepared by the incipient wetness impregnation of a support (fraction of  $0.125\text{--}0.250 \mu\text{m}$ ) with the solutions of corresponding salts, as which ammonium paramolybdate  $(\text{NH}_4)_6\text{Mo}_7\text{O}_{24} \cdot 4\text{H}_2\text{O}$  and cobalt nitrate  $\text{Co}(\text{NO}_3)_2 \cdot 4\text{H}_2\text{O}$  were used. The support was impregnated in two stages. After the first stage, the samples were dried in a drying oven at  $120^\circ\text{C}$  for 16 h; then, the temperature was increased to  $250^\circ\text{C}$  and the samples were additionally exposed for 4 h. After the second stage, the samples were dried at  $120^\circ\text{C}$  for 16 h and then calcined at  $550^\circ\text{C}$  for 4 h in an inert atmosphere. Then, the resulting oxide catalyst precursors were sulfidized. The catalysts were designated as Co–Mo/AMn.

The resulting samples were studied by physicochemical techniques.

**X-ray diffraction (XRD) analysis.** XRD analysis was performed on an ARL X'TRA diffractometer with monochromatic  $\text{CuK}_\alpha$  radiation ( $\lambda = 1.5418 \text{ \AA}$ ). The measurements were performed by point-by-point scanning in the  $2\theta$  range of angles from 10 to  $75^\circ$  at the scanning step  $\tau = 0.05^\circ$  and an accumulation time of 3–5 s at each point. Phase analysis was carried out by comparing the calculated values of interplanar spacing  $d_i$  and the corresponding intensities of diffraction peaks  $I_i$  with theoretical values from the JCPDS database (PCPDF Win. Ver. 1.30, JCPDS ICDD, Swarthmore, PA, USA, 1997).

**Texture characteristics.** The texture characteristics of the samples were determined on an ASAP-2400 instrument (Micromeritics) from the isotherms of low-temperature ( $-196^\circ\text{C}$ ) nitrogen adsorption; the samples were preliminarily kept in a vacuum at  $150^\circ\text{C}$ ; the error of the method was  $\pm 10\%$ .

**Surface acid–base properties.** The surface acid–base properties of the samples were studied by the IR spectroscopy of adsorbed probe molecules (CO and  $\text{CDCl}_3$ ) [16]. The IR spectra were recorded on a Shimadzu 8300 Fourier transform spectrometer in the range of  $1200\text{--}4000 \text{ cm}^{-1}$  with a resolution of  $4 \text{ cm}^{-1}$ ; 50 scans were accumulated for each spectrum. The samples were pressed as pellets with a density of  $(10\text{--}20) \times 10^{-3} \text{ g/cm}^2$  without a binding agent and evacuated in an IR cell to a residual pressure of  $< 10^{-4} \text{ Torr}$  at  $500^\circ\text{C}$  for 2 h.

Acid sites were determined using the adsorption of CO, which forms complexes with the Lewis and Brønsted acid sites (LASs and BASs, respectively). The adsorption of CO was conducted at a liquid nitrogen temperature ( $-196^\circ\text{C}$ ) and  $P_{\text{CO}} = 0.1\text{--}10 \text{ Torr}$ . An increase in the frequency of the vibrations of adsorbed CO relatively to the value for the gaseous molecule ( $v(\text{CO}) = 2143 \text{ cm}^{-1}$ ) was caused by the formation of complexes with LASs. The shift of the band  $v(\text{CO})$  to the region of high frequencies characterizes the strength of LASs because it is related to the heat of formation of complexes by the equation  $Q_{\text{CO}} [\text{kJ/mol}] = 10.5 + 0.5(v(\text{CO}) - 2143)$ . The concentration of LASs was measured from the integrated intensity of bands due to adsorbed CO (in the spectral region of  $2185\text{--}2240 \text{ cm}^{-1}$ ) using the formula  $N[\mu\text{mol/g}] = A/A_0$ , where  $A$  is the integrated intensity of the band of adsorbed CO, and  $A_0$  is the integral absorption coefficient [16].

Basic sites (BSs) were determined using the adsorption of deuteriochloroform ( $\text{CDCl}_3$ ). Deuterochloroform was adsorbed at  $0^\circ\text{C}$  and a pressure equal to the pressure of  $\text{CDCl}_3$  vapor at  $20^\circ\text{C}$ . The decomposition of CD bands in  $\text{CDCl}_3$  was performed taking into account the following considerations: (1) the minimization of the number of bands, (2) the Gaussian line shape, and (3) the broadening of absorption bands upon shifting to the region of low frequencies.

The IR spectra were normalized to the pellet density. The accuracy of concentration measurements was  $\pm 15\%$ .

**Electron microscopic studies.** The electron microscopic studies of the samples were conducted on a JEM-2010 transmission electron microscope (JEOL) (resolution,  $0.14 \text{ nm}$ ; accelerating voltage,  $200 \text{ kV}$ ). Local energy-dispersive x-ray analysis (EDX), which was carried out on an EDAX spectrometer (EDAX Co.), was used for determining the concentrations of elements and ratios between them. The test samples

were supported onto a carbon substrate immobilized on copper gauze.

**X-ray photoelectron spectroscopy (XPS).** The X-ray photoelectron spectra of Co–Mo/AMn were obtained on a SPECS spectrometer using  $AlK_{\alpha}$  radiation ( $h\nu = 1486.6$  eV). The samples were supported onto double-sided conducting copper Scotch tape. The C1s line (284.8 eV) from carbon, which was present on the catalyst surface, was used for calibration. Survey spectra were written at a transmission energy of 50 eV; individual sections were written at 20 eV. The relative concentrations of elements on the catalyst surfaces and the ratios between their atomic concentrations were determined from the integrated intensities of photoelectron lines corrected for the appropriate atomic sensitivity coefficients [17].

**Catalytic activity.** The activity of catalysts in the reactions of dibenzothiophene (DBT), 4-methyldibenzothiophene (4-MDBT), and 4,6-dimethyldibenzothiophene (4,6-DMDBT) hydrodesulfurization was determined in a 300-ml batch reactor (Autoclave Engineers type Magne-Drive), which was equipped with a system for sampling liquids at regular intervals in the course of reaction. The experiments were carried out at a hydrogen pressure of 3.5 MPa, 340°C, and 1000 rpm; the duration of the experiments was 6 h. For determining the catalytic activity, 3 g of a catalyst and 150 ml of a reaction mixture were used in each particular cycle. Test samples were taken at regular intervals of 1 h.

The reaction mixture containing 500 ppm of DBT, 250 ppm of 4-MDBT, and 80 ppm of 4,6-DMDBT was prepared by the dissolution of the model substances in diesel fuel, which was obtained as a result of the hydrofining of straight-run gas oil containing 8 ppm of S, 7 ppm of N, and mono-, di-, and polycyclic aromatic compounds (21.7, 1.89, and 0.81 wt %, respectively). In order to eliminate the effect  $H_2S$  on the activity of the samples, an excess amount of dimethyl disulfide, which corresponded to 1.2 wt % sulfur, was added to the reaction mixture. Under these conditions, the absence of external and/or internal diffusion limitations was confirmed by additional experiments. In an individual series of experiments performed with catalyst fractions of 0.08–0.125, 0.125–0.18, 0.18–0.25, and 0.25–0.50 mm under the same conditions, we found that the catalyst activity does not depend on particle size in the range of 0.08–0.25 mm; this suggests the kinetic region of the reaction.

Before testing the catalysts, their oxide precursors were sulfidized in a tube reactor at 400°C for 4 h in a flow of 10 vol %  $H_2S$  in  $H_2$  at atmospheric pressure.

The concentrations of the sulfur-containing compounds (DBT, 4-MDBT, and 4,6-DMDBT) in the test samples were determined by gas chromatography with the use of an Agilent 6890N chromatograph equipped

with a JAS atomic-emission detector (from the emission line of sulfur atoms at 181 nm). The components were separated on an HP-1MS capillary column (60.0 m × 250  $\mu$ m × 1.00  $\mu$ m). The rate constants were calculated from the pseudo-first-order equation with respect to the concentration of sulfur-containing compounds:

$$K_i = \frac{-\ln(1-x)}{t},$$

where  $x$  is conversion,  $t$  is time, and  $i$  refers to DBT, 4-MDBT, or 4,6-DMDBT.

## RESULTS AND DISCUSSION

### *Characteristics of the Supports*

**Phase composition and texture.** According to XRD data (Fig. 1), samples AMn containing 1 and 5 mol %  $M_xO_y$  calcined at 550°C are X-ray amorphous; that is, the modification of aluminum oxide with the specified components leads to its amorphization regardless of the nature and concentration of the introduced additive.

Table 1 summarizes the texture characteristics aluminum oxide modified with Sr, Ba, and La cations and calcined at 550°C. It is evident that the introduction of 1 mol %  $M_xO_y$  considerably decreased the specific surface area of the modified samples (AS1, AB1, and AL1; 135–200  $m^2/g$ ), as compared with aluminum oxide (A, 300  $m^2/g$ ). Simultaneously, an insignificant decrease in the pore volume from 1.00  $cm^3/g$  for sample A to 0.85  $cm^3/g$  for AS1 and AL1 was observed; in this case, the mean pore diameter increased from 14 nm for  $Al_2O_3$  to 17.5–25.5 nm in the modified samples.

An increase in the concentration of a modifying additive to 5 mol %  $M_xO_y$  resulted in a further decrease in the specific surface area of modified samples AS5 and AL5 (115–120  $m^2/g$ ) (Table 1); furthermore, the pore volume further decreased. Barium-modified sample AB5 is the exception: the specific surface area and pore volume remained almost the same as those upon the introduction of 1 mol % BaO (Table 1). A possible reason for the observed effect is that barium carbonate is formed as the fraction of barium in the sample is increased. Barium carbonate is characterized by insignificant degree of dispersion; consequently, it does not exert a noticeable effect on the texture characteristics of the sample.

**Acid–base properties of the supports.** Figure 2 shows the spectra of the samples after evacuation at 500°C. In the spectra of samples AS1, AS5, AB1, AB5, AL1, and AL5, absorption bands at 1380–1480 and 2340  $cm^{-1}$  indicate the presence of the carbonate ion  $CO_3^{2-}$  and  $CO_2$ , respectively (it is likely that the latter was due to the encapsulation of  $CO_2$  in closed

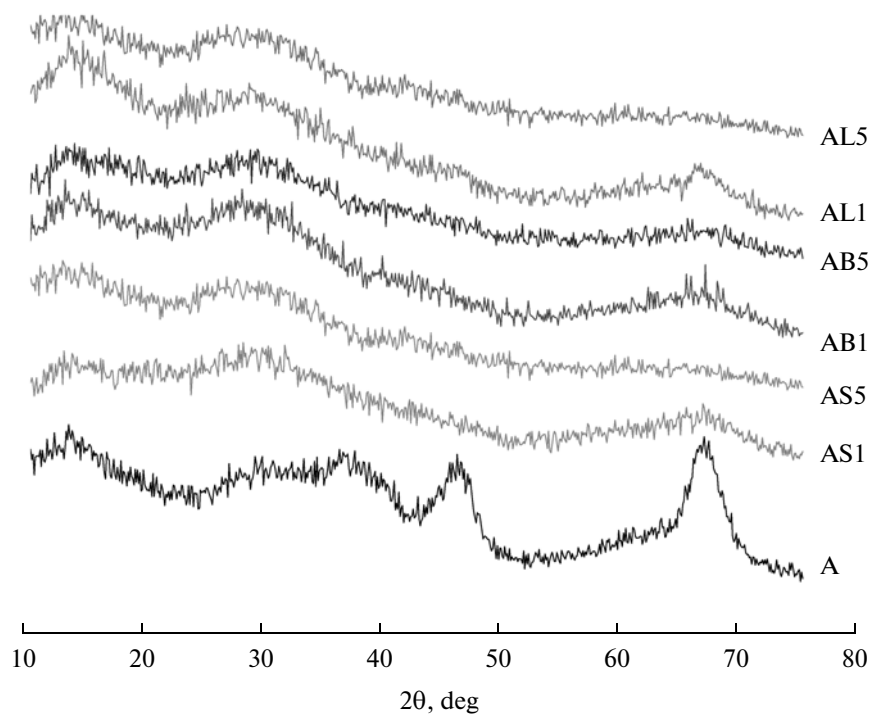


**Fig. 1.** Diffraction patterns of aluminum oxide modified with cations of alkaline-earth and rare-earth elements.

pores). These structures were absent from the spectrum of the parent aluminum oxide. We can conclude that carbonate species are formed on the surface of the modified samples. Therefore, the modification of the  $\text{Al}_2\text{O}_3$  surface with alkaline-earth or rare-earth metal ions leads to a considerable increase in the number of basic sites, which are sufficiently strong to interact with  $\text{CO}_2$  at room temperature.

In the spectrum of  $\text{Al}_2\text{O}_3$  in the region of hydroxyl groups, absorption bands due to the vibrations of hydroxyl groups ( $\nu(\text{OH})$ ) were observed at 3680, 3730,

3770, and  $3785\text{ cm}^{-1}$ . The samples modified with alkaline-earth or rare-earth metal ions exhibited a considerable decrease in the intensity of the corresponding bands. Furthermore, it is likely that an absorption band at  $3600\text{ cm}^{-1}$  was due to the presence of an  $\text{M}-\text{OH}$  bond in the modified samples.

According to data given in Table 2, the total concentration of OH groups decreases in the following order:

sample μmol/g	A	AL1	AS1	AB1	AS5	AB5	AL5
675	348	232	229	205	187	175.	

**Table 1.** Texture characteristics of the supports according to data on low-temperature nitrogen adsorption

Sample	Modifier and its concentration		Designation	$S_{\text{BET}}$ , $\text{m}^2/\text{g}$	$V_{\text{pore}}$ , $\text{cm}^3/\text{g}$	$D_{\text{av}}$ , nm
	M	$\text{M}_x\text{O}_y$ , mol %				
$\text{Al}_2\text{O}_3$	—	—	A	300	1.00	14.0
$\text{Al}_2\text{O}_3-\text{SrO}(1)$	Sr	1	AS1	135	0.85	25.5
$\text{Al}_2\text{O}_3-\text{BaO}(1)$	Ba		AB1	155	1.00	25.0
$\text{Al}_2\text{O}_3-\text{La}_2\text{O}_3(1)$	La		AL1	200	0.85	17.5
$\text{Al}_2\text{O}_3-\text{SrO}(5)$	Sr	5	AS5	115	0.65	22.5
$\text{Al}_2\text{O}_3-\text{BaO}(5)$	Ba		AB5	155	0.90	22.5
$\text{Al}_2\text{O}_3-\text{La}_2\text{O}_3(5)$	La		AL5	120	0.55	19.0

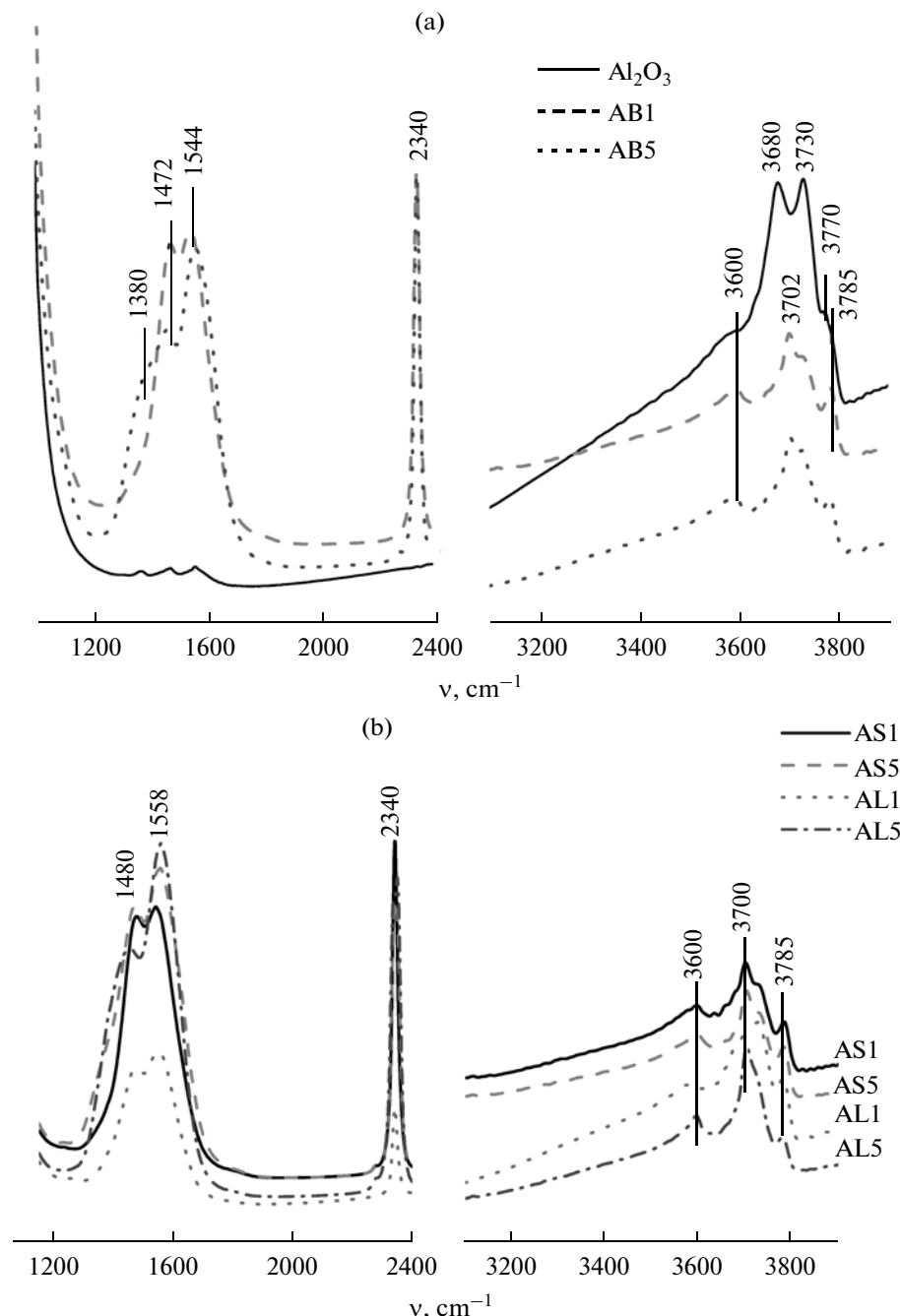


**Fig. 2.** IR spectra of support samples after evacuation at 500°C: (a)  $\text{Al}_2\text{O}_3$ , AB1, and AB5; (b) AS1, AS5, AL1, and AL5.

In this case, the total concentration of terminal ( $3700\text{--}3790 \text{ cm}^{-1}$ ) and bridging ( $3660\text{--}3680 \text{ cm}^{-1}$ ) OH groups changed in the following order:

$$\begin{aligned} C_{\text{term}} & \text{ A} > \text{AL1} > \text{AB5} > \text{AS1} > \text{AL5} > \text{AS5} > \text{AB1} \\ C_{\text{bridg}} & \text{ A} > \text{AL1} > \text{AS1} > \text{AL5} > \text{AB5} > \text{AB1} > \text{AS5}. \end{aligned}$$

Note that the concentration of bridging OH groups in the modified samples was much lower than that in the parent aluminum oxide; in this case, differences

caused by the nature and concentration of the modifier additive were insignificant (Table 2).

Figure 3 shows the spectra of adsorbed CO in the regions of  $\nu(\text{CO})$  and hydroxyl groups; the pressure of CO was changed from 0.1 to 10 Torr. In the spectra of CO adsorbed on the samples modified with  $\text{M}_x\text{O}_y$ , an absorption band appeared at  $2165\text{--}2175 \text{ cm}^{-1}$  (Fig. 3) due to CO complexes with weaker LASs (as compared with  $\text{Al}_2\text{O}_3$ ); this absorption band did not manifest itself in the spectra of CO on  $\text{Al}_2\text{O}_3$ . It is likely that it

**Table 2.** Positions of absorption band maximums due to support hydroxyl groups and concentrations of these groups

Sample	$\nu, \text{cm}^{-1}$							$\Sigma \text{OH}$ ( $C_{\text{term}}/C_{\text{bridg}}$ )
	3660–3665	3670–3680	3700–3710	3730	3750	3773	3790	
	Concentration of OH groups, $\mu\text{mol/g}$							
A	132	176	58	163	80	35	31	675 (367/308)
AS1	28	11	71	41	56	—	24	232 (193/39)
AB1	12	20	76	43	33	—	45	229 (197/32)
AL1	10	41	105	77	77	—	38	348 (297/51)
AS5	17	11	65	39	50	—	24	205 (178/28)
AB5	9	22	48	45	63	—	—	187 (156/31)
AL5	24	9	75	46	44	—	21	175 (186/33)

**Table 3.** Positions of absorption band maximums due to CO adsorbed on the supports and the concentrations of LASs

Sample	$\nu, \text{cm}^{-1}$				$\Sigma \text{LASs}, \mu\text{mol/g}$ ( $\mu\text{mol/m}^2$ )
	2165–2175	2185–2200	2214	2225	
	Concentration of LASs, $\mu\text{mol/g}$ ( $\mu\text{mol/m}^2$ )				
A	—	625 (2.08)	7.2 (0.03)	4 (0.01)	636 (2.12)
AS1	125 (0.91)	212 (1.55)	16 (0.12)	—	353 (2.58)
AB1	62 (0.40)	188 (1.20)	8 (0.12)	—	268 (1.70)
AL1	112 (0.56)	269 (1.35)	14.5 (0.07)	—	395 (1.98)
AS5	188 (1.61)	125 (1.07)	13.6 (0.12)	—	327 (2.79)
AB5	125 (0.79)	162 (1.02)	23 (0.14)	—	310 (1.95)
AL5	375 (3.12)	88 (0.73)	11 (0.09)	—	474 (3.95)

belongs to the complexes of CO with the coordinatively unsaturated modifying ions  $\text{Sr}^{2+}$ ,  $\text{Ba}^{2+}$ , and  $\text{La}^{3+}$ . Furthermore, the intensity of bands in the region of 2185–2200  $\text{cm}^{-1}$  for the modified samples was much lower than that for  $\text{Al}_2\text{O}_3$ , and, on the contrary, the intensity of bands at 2214  $\text{cm}^{-1}$  was higher. The absorption band with a frequency of 2225  $\text{cm}^{-1}$ , which characterizes strong LASs, in the spectrum of CO on

$\text{Al}_2\text{O}_3$  has a low intensity, and it does not appear in the spectra of CO on the modified samples.

Table 3 summarizes the concentrations of LASs of different strengths and the total concentrations of LASs in the test samples. The experimental data suggest that the concentration of LASs (on a square meter basis) corresponding to an absorption band at 2165–2175  $\text{cm}^{-1}$  decreases in the order AL5 > AS5 > AS1  $\approx$

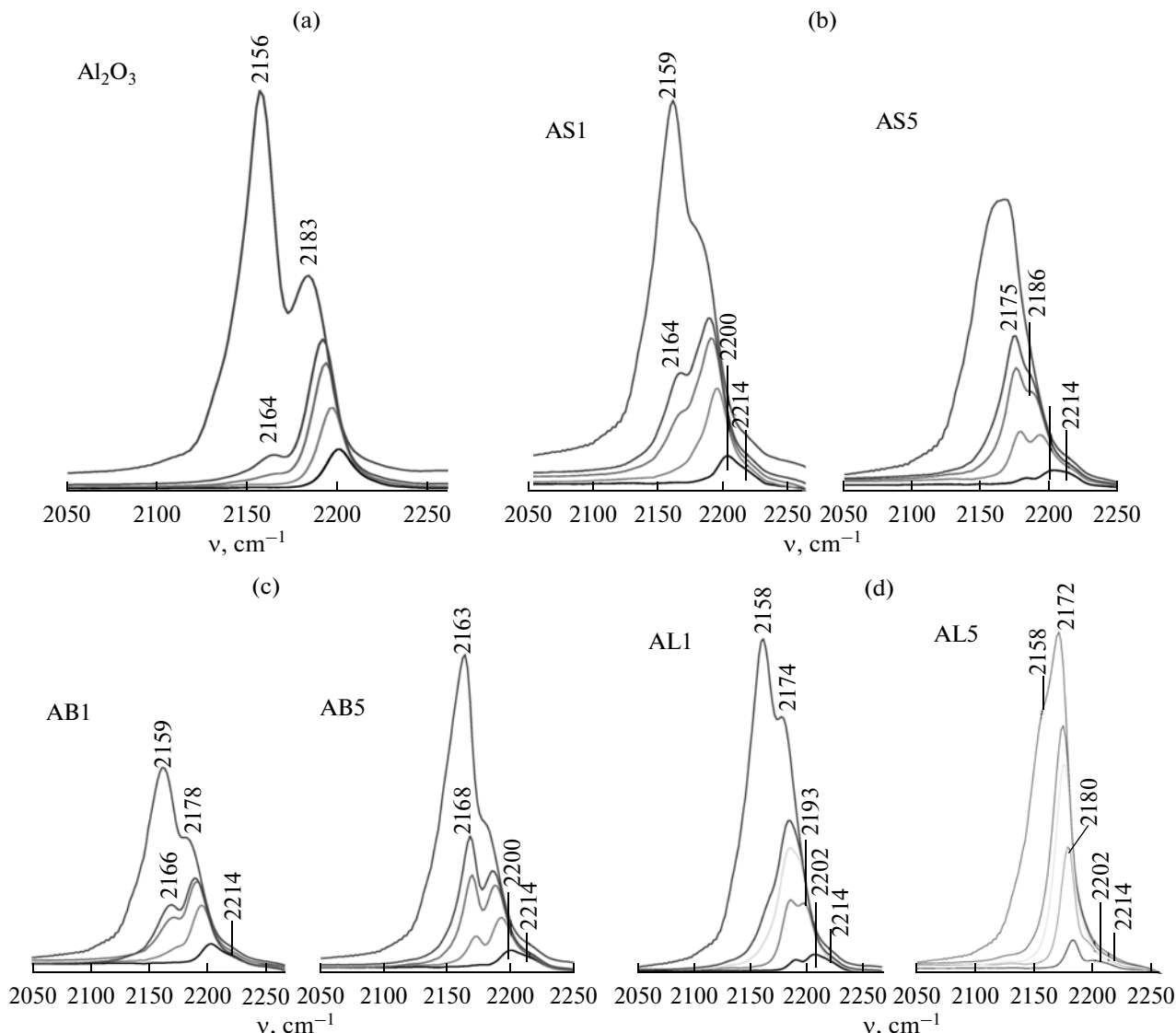


**Fig. 3.** IR spectra of CO adsorbed on the following supports at pressures changed from 0.1 to 10 Torr: (a)  $\text{Al}_2\text{O}_3$ , (b) AS1 and AS5, (c) AB1 and AB5, and (d) AL1 and AL5.

$\text{AB}5 > \text{AL}1 > \text{AB}1$ ; that is, the smallest concentration of these sites is observed in the samples modified with barium. This is additional evidence for the fact that barium primarily interacts with  $\text{CO}_2$  to form carbonate and, to a lesser degree, with  $\text{Al}_2\text{O}_3$  at  $550^\circ\text{C}$ . The concentration of LASs (on a square meter basis) corresponding to an absorption band at  $2185\text{--}2200\text{ cm}^{-1}$  decreases in the order  $\text{A} > \text{AS}1 > \text{AL}1 > \text{AB}1 > \text{AS}5 > \text{AB}5 > \text{AL}5$ . Consequently, the introduction of modifying additives and an increase in their fraction facilitate the monotonic decrease in the concentration of these LASs. The concentration of LASs (on a square meter basis) corresponding to an absorption band at  $2214\text{ cm}^{-1}$  decreases in the order  $\text{AB}5 > \text{AS}1 \approx \text{AB}1 \approx \text{AS}5 > \text{AL}5 > \text{AL}1 > \text{A}$ ; in this case, it varies in the

range of  $0.03\text{--}0.14\text{ }\mu\text{mol/m}^2$  (Table 3). The total concentrations of LASs ( $\Sigma\text{LASs}$ ) (on a square meter basis) changes as follows:  $\text{AL}5 > \text{AS}5 > \text{AS}1 > \text{A} > \text{AL}1 \approx \text{AB}5 > \text{AB}1$ . Thus, the modification aluminum oxide with the cations of alkaline-earth and rare-earth elements leads to the appearance of weaker LASs and a decrease in the concentration of medium-strength LASs. Furthermore, the total concentration of LASs increases upon the introduction of strontium and lanthanum cations into  $\text{Al}_2\text{O}_3$  and decreases upon the introduction of barium cations.

The basicity of samples was characterized using the spectra of adsorbed deuterochloroform (Fig. 4). Deuterated chloroform forms hydrogen bonds with surface BSs. As the strength of sites increased, the frequency

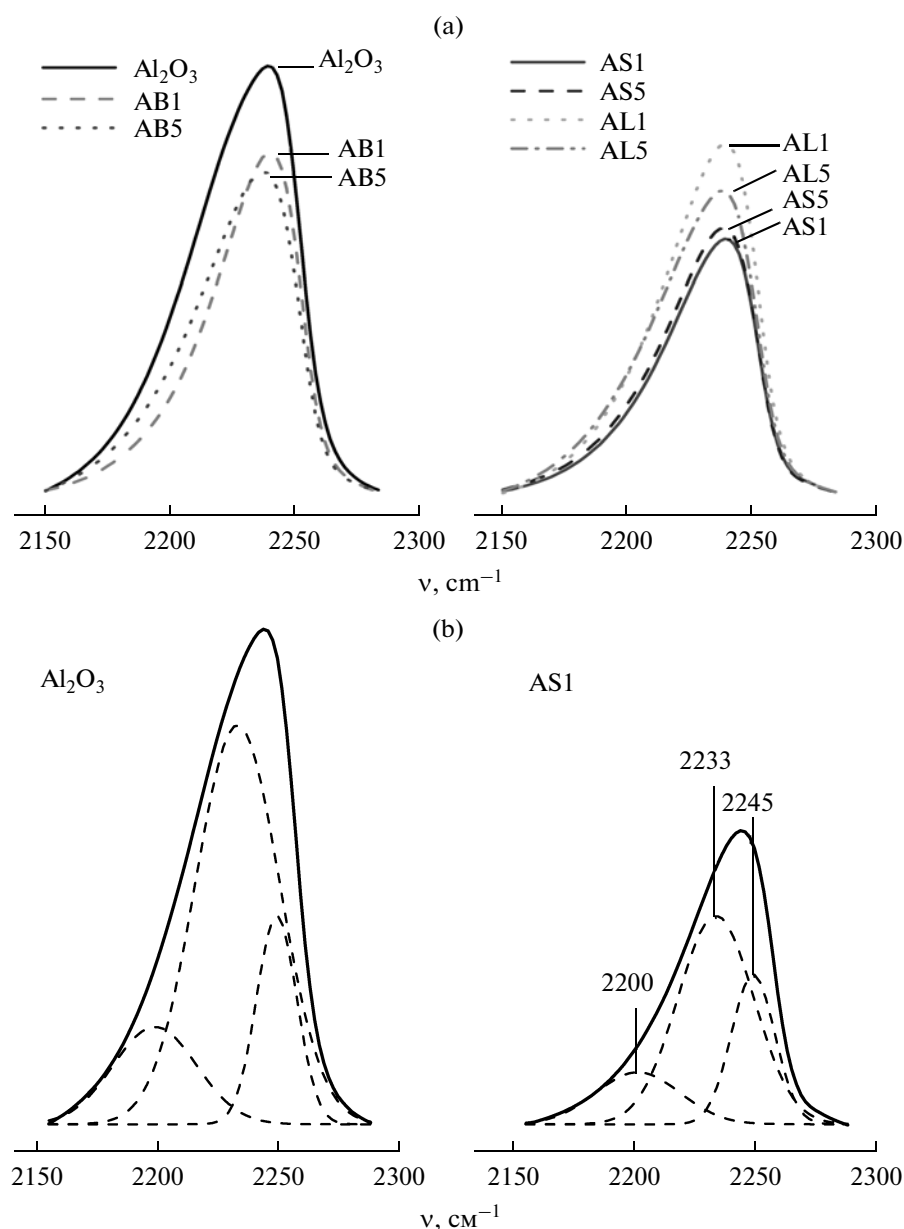


**Fig. 4.** (a) IR spectra of  $\text{CDCl}_3$  adsorbed on aluminum oxide and modified samples; (b) examples of the deconvolution of the spectrum of  $\text{CDCl}_3$  adsorbed on  $\text{Al}_2\text{O}_3$  and AS1.

of an absorption band due to the C—D bond decreased. Three components can be recognized in the spectra of adsorbed  $\text{CDCl}_3$  (Fig. 4b); they correspond to BSs of different strengths. The first, second, and third ones components with  $\nu(\text{CD}) = 2245$ , 2227–2233, and  $2200 \text{ cm}^{-1}$  have strengths of 860, 890, and 930 kJ/mol, respectively. Table 4 summarizes the concentrations of the strongest BSs, for which  $\text{PA} = 930 \text{ kJ/mol}$ , and the total concentrations of BSs. The surface concentration of strong BSs (on a square meter basis) increases in the order  $\text{A} < \text{AL1} < \text{AB5} < \text{AS1} < \text{AB1} < \text{AL5} \approx \text{AS5}$ ; that is, the introduction of modifying additives leads to an increase in the concentration

of strong BSs. In this case, the greatest effect is achieved upon the introduction of strontium and lanthanum rather than barium cations into  $\text{Al}_2\text{O}_3$ . This result is somewhat unexpected, if one takes into account the electronegativity values of the introduced cations of alkaline-earth and rare-earth elements [18], according to which barium is characterized by the greatest basicity. It is likely that a lowered concentration of strong BSs on the surfaces of samples ABn is caused by the fact that they easily interact with atmospheric  $\text{CO}_2$  with the formation of surface carbonate species, and they cannot be detected in a study with probes like  $\text{CDCl}_3$ . Weaker BSs, which are close to the

surface sites of  $\text{Al}_2\text{O}_3$  in strength, slowly react with atmospheric carbon dioxide.

According to data given in Table 4, the total concentration of BSs on the surface of the samples under investigation changes in the order AL5 > AS5 > AB1 > AB5 > AL1  $\approx$  AS1 > A. The found total concentrations of BSs on the surfaces of the specified samples are comparable in the absolute value with the total concentration of LASs (Table 3).

#### Catalyst Characterization

Pure aluminum oxide and  $\text{Al}_2\text{O}_3$  modified with the cations of alkaline-earth and rare-earth elements in amounts of 1 and 5 mol % were used as supports for Co–Mo hydrodesulfurization catalysts. The concentrations of active components in the catalysts were  $(6 \pm 0.2)$  wt % CoO and  $(19 \pm 0.2)$  wt %  $\text{MoO}_3$ . The resulting Co–Mo catalysts were characterized after performing a hydrodesulfurization process.

**High-resolution transmission electron microscopy (HRTEM).** According to electron-microscopic data, the support of sample Co–Mo/A has a spongy (block/mesoporous) morphology and consists of agglomerated partially coalesced isometric crystallites with a characteristic size of  $\sim 7$  nm. The active component as Co–Mo–S sulfide packets is located on the surface of  $\text{Al}_2\text{O}_3$  particles and has a diameter of 5–7 nm and a thickness from one (predominantly) to three monolayers (more rarely) (Fig. 5).

The morphology of the support particles of sample Co–Mo/AS1 (Fig. 6) differed from the above in an increase in the porosity (the observed mesopore size was about 5 nm). Taking into account the results of XRD analysis, we can assume that a modifying additive (strontium) partially interacts with aluminum oxide. Another portion of strontium forms the oxide  $\text{SrO}$ , whose particle size is as great as 10 nm (Fig. 6).

**Table 4.** Positions of absorption band maximums due to  $\text{CDCl}_3$  adsorbed on the supports and the concentrations of BSs

Sample	Concentration of BSs, $\mu\text{mol/g}$ ( $\mu\text{mol/m}^2$ ) – ( $v, \text{cm}^{-1}$ )	$\Sigma$ BSs, $\mu\text{mol/g}$ ( $\mu\text{mol/m}^2$ )
A	50 (0.17) – (2198)	530 (1.8)
AS1	40 (0.29) – (2200)	293 (2.1)
AB1	48 (0.31) – (2205)	390 (2.5)
AL1	40 (0.20) – (2200)	423 (2.1)
AS5	40 (0.34) – (2202)	300 (2.6)
AB5	42 (0.26) – (2198)	383 (2.4)
AL5	40 (0.33) – (2198)	366 (3.1)

The Co–Mo–S sulfide packets of this sample are identical to those of sample Co–Mo/A in terms of morphology; however, their degree of dispersion is higher. The particle size distribution of Co–Mo–S shows an increase in the number of islets with diameters to 2 nm.

The morphology and particle size of sample Co–Mo/AB1 (Fig. 7) are almost identical to those of sample Co–Mo/AS1 (Fig. 6). However, in this sample, a portion of barium unreacted with aluminum oxide forms a highly dispersed Ba-containing compound with the particle sizes of 2–3 nm (Fig. 7c), which manifests itself in an increase in the concentration of this compound. In this case, large  $\text{BaO}$  particles were not detected in the sample. According to EDX analysis data, the concentrations of Ba determined in different chosen sections (Figs. 7a, 7b) proved to be the same (Fig. 7d) and equal to 0.88–0.84 at % at an Al concentration of 99.16–99.12 at %.

For sample Co–Mo/AL1, the morphology of support particles and the morphology and size of Co–Mo–S sulfide packets (Fig. 8a) are analogous to those

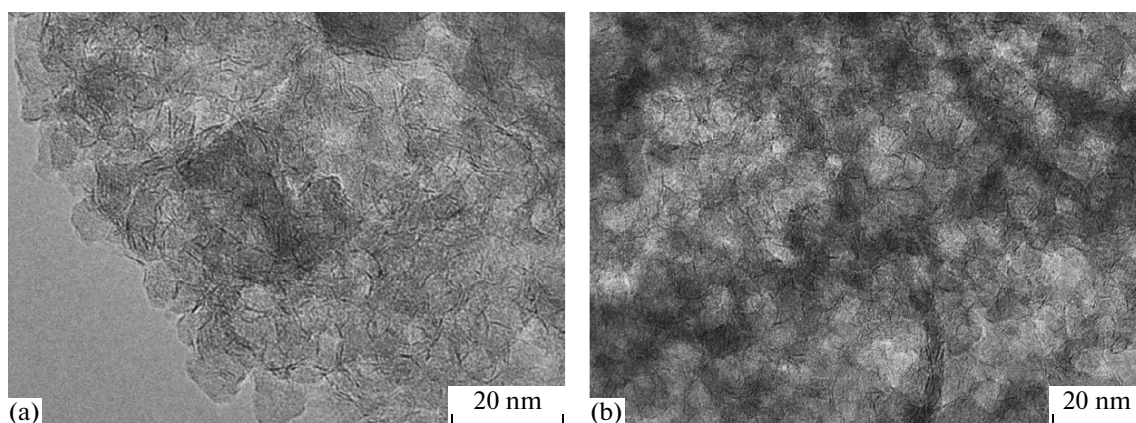


**Fig. 5.** HRTEM images of (a, b) different areas of Co–Mo/A.

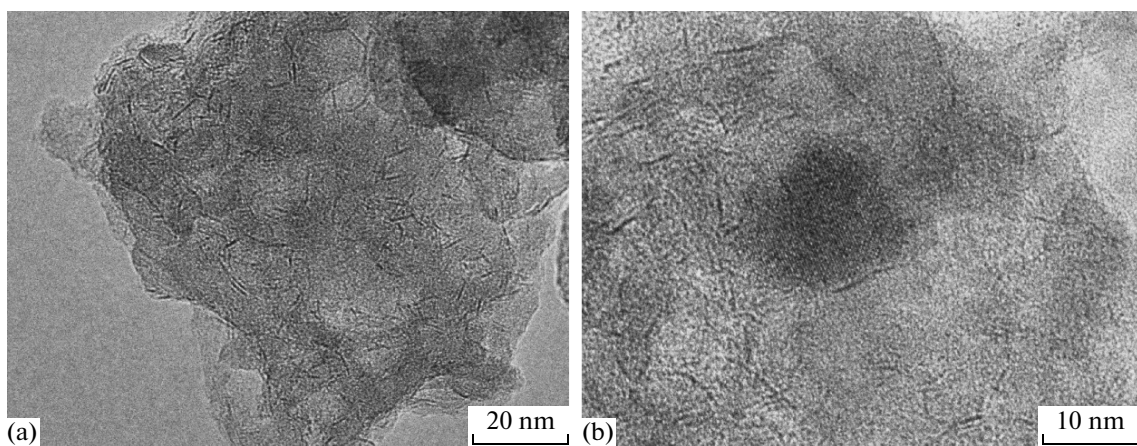


**Fig. 6.** HRTEM images of Co–Mo/AS1: (a) sulfide packets on the catalyst surface and (b) formation of SrO particles.

in sample Co–Mo/A. However, large particles ( $\sim 10$  nm) (Fig. 8b), were present in this sample; according to EDX-analysis data, these particles can be attributed to the oxide compounds of La. Consequently, the promotion of aluminum oxide with lanthanum does not change the morphology and particle size of  $\text{Al}_2\text{O}_3$ , but it is accompanied by the formation of bulky large La-containing particles. The sizes of Co–Mo–S sulfide packets located on the surface of the large oxide La-containing particles are increased: the diameters are as great as 20 nm, and the thickness is to five sulfide layers. This can suggest that the introduction of La leads to a strengthening of the bond of a sulfide component with the modified support.

**X-ray photoelectron spectroscopy (XPS).** For the catalysts prepared with the use of unmodified aluminum oxide and aluminum oxide modified with 1 mol %  $\text{M}_x\text{O}_y$ , XPS spectra were measured in the spectral regions corresponding to the binding energies of elements present in the samples ( $\text{Al} 2p$ ,  $\text{S} 2p$ ,  $\text{Mo} 3d_{5/2}$ ,

$\text{C} 1s$ ,  $\text{O} 1s$ ,  $\text{Co} 2p_{3/2}$ ,  $\text{Sr} 3d_{5/2}$ ,  $\text{Ba} 3d_{5/2}$ , and  $\text{La} 3d_{5/2}$ ) in order to determine their chemical states (Table 5). The comparison of the binding energies of the corresponding elements indicates that the values of  $E_b$  ( $\text{Al} 2p$ , ( $\text{Al} 2s$ ), ( $\text{S} 2p$ ), ( $\text{C} 1s$ ), and ( $\text{O} 1s$ ) are 74.7, 119.5, 162.3, 284.8, and 531.7 eV, respectively, regardless of the nature of the catalyst.

From an analysis of the  $\text{S} 2s + \text{Mo} 3d_{5/2}$  XPS spectra of the test samples (Fig. 9), it follows that a peak with the lowest binding energy ( $E_b = 226.3$  eV) belongs to sulfur (the  $\text{S} 2s$  level). In order to more accurately determine the ratio between the sulfide and oxide forms of molybdenum, we performed the deconvolution of the  $\text{Mo} 3d_{5/2}$  line into individual spectral components with the use of the XPS-Peak software taking into account the contribution of  $\text{S} 2s$  peaks to the total  $\text{S} 2s + \text{Mo} 3d_{5/2}$  spectrum (Fig. 9). The  $\text{Mo} 3d_{5/2}$  spectrum exhibited two main peaks with  $E_b = 229.2$  and 232.8 eV, which can be attributed to molybdenum in a sulfide environment (for example, in the compound

**Table 5.** Binding energies for the elements in catalyst samples according to XPS data

Sample	$E_b$ , eV									
	$\text{Al} 2p$	$\text{Al} 2s$	$\text{S} 2p$	$\text{Mo} 3d$	$\text{C} 1s$	$\text{O} 1s$	$\text{Co} 2p$	$\text{Sr} 3d$	$\text{Ba} 3d$	$\text{La} 3d$
Co–Mo/A	74.7	119.6	162.4	229.2	284.8	531.7	779.3 782.0	—	—	—
Co–Mo/AS1	74.7	119.5	162.3	229.2	284.8	531.7	779.2 781.9	134.5	—	—
Co–Mo/AB1	74.7	119.5	162.3	229.1	284.8	531.7	779.4	—	780.6	—
Co–Mo/AL1	74.7	119.6	162.3	229.1	284.8	531.7	779.3 781.9	—	—	835.7

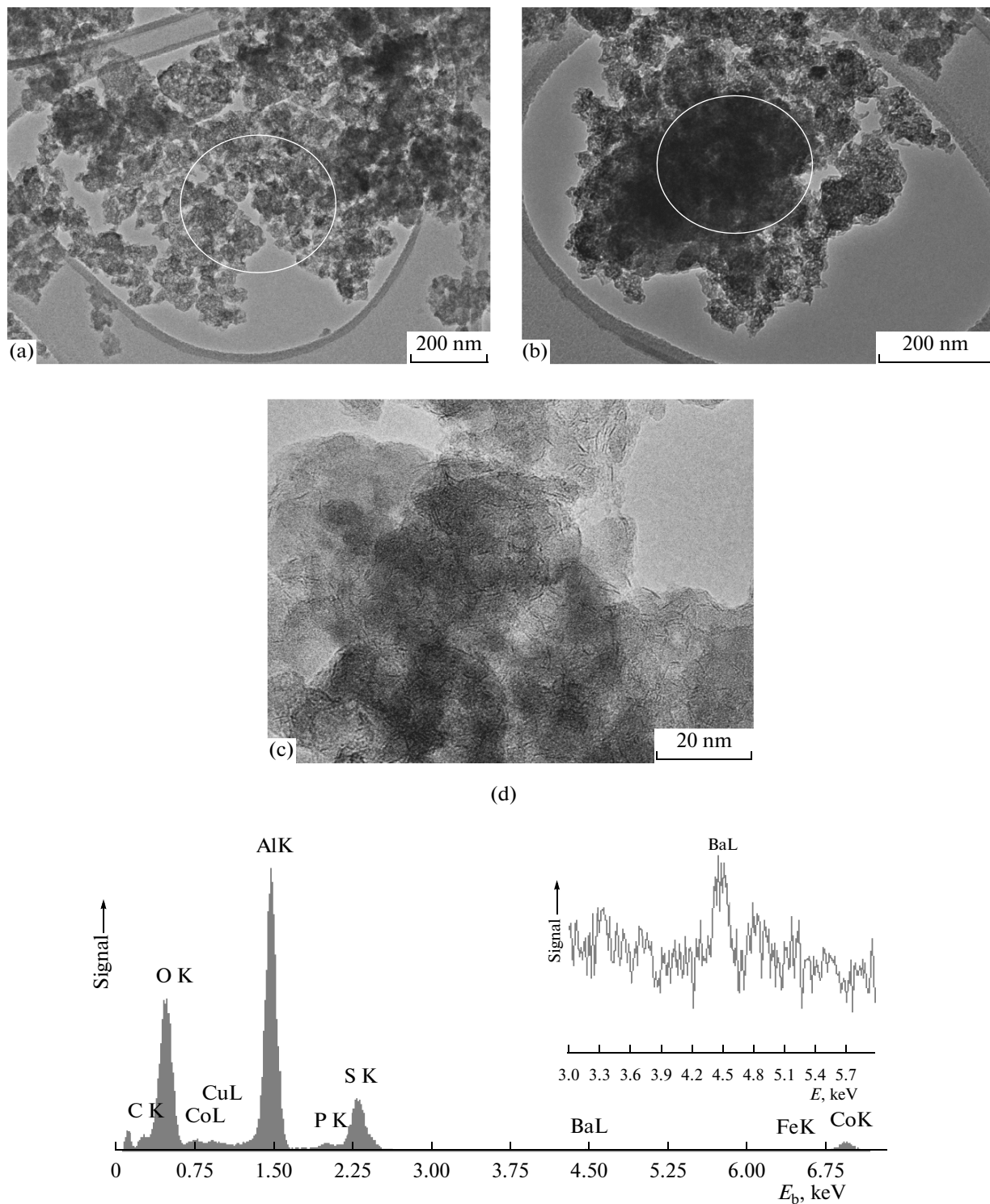


**Fig. 7.** HRTEM images of Co–Mo/AB1: (a, b) EDX analysis areas, (c) sulfide packets on the catalyst surface, and (d) EDX analysis (see the text for details).

$\text{MoS}_2$ ), where the formal state of molybdenum is  $\text{Mo}^{4+}$ , and to molybdenum in the state  $\text{Mo}^{6+}$  in an oxygen environment, respectively (for example,  $\text{MoO}_3$ ,  $\text{Al}_2(\text{MoO}_4)_3$ , or  $\text{CoMoO}_4$ ) [19–23].

The  $\text{Co } 2p_{3/2}$  XPS spectra of the test samples (Fig. 10) also contain two peaks with the binding energies of 779.2 and 782.0 eV; the smaller value ( $779.1 \pm 0.1$  eV) is characteristic of cobalt in a sulfide environment, and

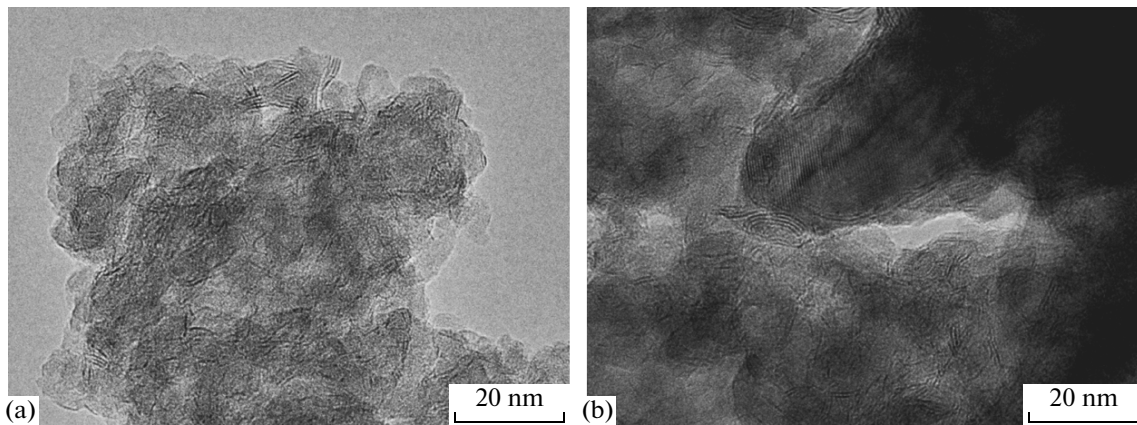


**Fig. 8.** HRTEM images of Co–Mo/AL1: (a) sulfide packets on the catalyst surface and (b) formation of lanthanum oxide particles.

the greater value ( $782.0 \pm 0.1$  eV) is characteristic of the state  $\text{Co}^{2+}$  in an oxygen environment [19–23]. It should be noted that, for sample Co–Mo/AB1, the analysis of the chemical state of cobalt is considerably difficult to perform as a result of the overlapping of Co  $2p$  and Ba  $3d$  peaks. Figure 11 shows the spectra of the catalyst and support containing BaO and the difference spectrum normalized to the Al  $2p$  peak intensity. We found that the qualitative pattern obtained after the measurement of the difference spectrum was approximately the same as that for the other samples; however, the ratio between the sulfide and oxide forms of cobalt cannot be reliably determined.

Some difficulties appear in the identification of strontium in sample Co–Mo/AS1 as a result of the low intensity of photoelectron peaks characteristic of strontium (Fig. 12). The binding energy of Sr  $3d_{5/2}$  is

134.5 eV. According to published data [24–30], the binding energy of Sr  $3d_{5/2}$  lies in the ranges of 131.7–132.4, 132.8, 133.4–133.8, and 133.6–134.1 eV for strontium as the constituent of SrO,  $\text{Sr(OH)}_2$ ,  $\text{SrCO}_3$  and strontium hydroxo carbonates, respectively. Consequently, the observed peak can be attributed to a hydroxo carbonate form of strontium [24, 25].

For all of the test samples, the S  $2p$  spectrum (Fig. 13) exhibited two peaks with the binding energies of  $162.2 \pm 0.2$  and 169.3 eV. The binding energy of the former peak is characteristic of sulfide ions (sulfur is in the state  $\text{S}^{2-}$ ), and that of the latter peak is characteristic of sulfate ions ( $\text{SO}_4^{2-}$ ), which are likely bound to aluminum in the form of  $\text{Al}_2(\text{SO}_4)_3$  [22, 31, 32]. It is evident from the above spectra that the fractions of sulfide ( $S_d$  is sulfide) and sulfate ( $S_t$  is sulfate) states of

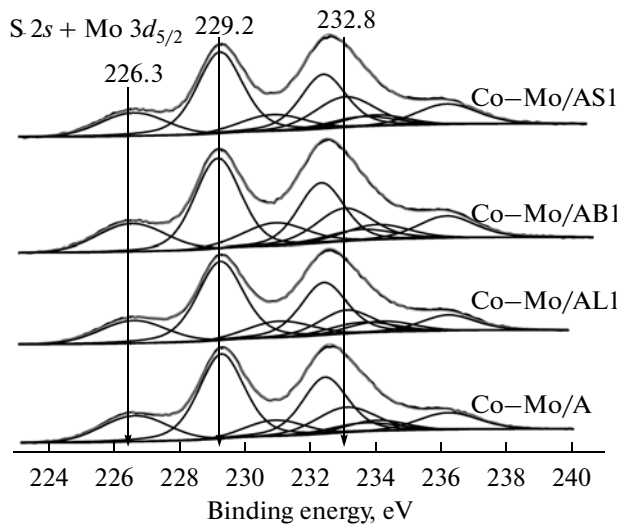


**Fig. 9.** The Mo  $3d_{5/2}$  XPS spectra of Co–Mo/AM1 samples and the decomposition of lines into individual spectral components.

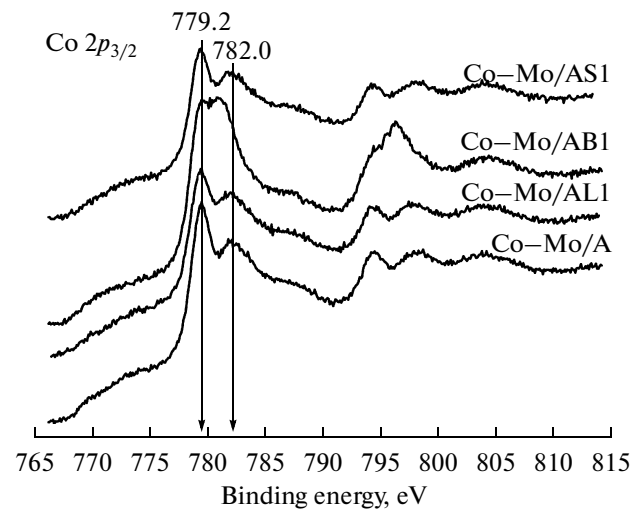


**Fig. 10.** The Co  $2p_{3/2}$  XPS spectra of Co–Mo/AM1 samples.

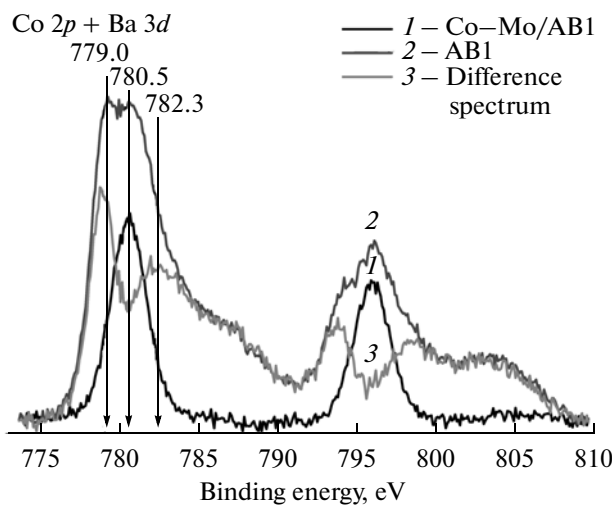


**Fig. 11.** The Co 2p<sub>3/2</sub> XPS spectra of AB1 samples and Co-Mo/AB1 (see the text for details).

sulfurs are different in different samples, and the ratio S<sub>d</sub>/S<sub>t</sub> varies over the range of 1.96–2.50 (Table 6).

The relative concentrations of the elements on the catalyst surfaces and the ratios between atomic concentrations were determined from the integrated intensities of lines in the XPS spectra corrected for the appropriate atomic sensitivity coefficients. According to the experimental results (Table 6), the Co : Mo surface ratio decreases in the following order of the catalysts: Co–Mo/A > Co–Mo/AL1 ≈ Co–Mo/AB1 > Co–Mo/AS1. The fraction of the sulfide form of molybdenum (Mo<sup>4+</sup>/Mo<sub>total</sub>) decreases in the same order. In this case, the Mo : Al, O : Al, and S : Al surface ratios are almost independent of the nature of the modifying additive and change within the limits of experimental error.

**Catalytic activity tests.** Table 7 lists the rate constants of the hydrodesulfurization reaction for three model substances and seven catalysts. According to the results obtained, an increase in the rate constants of conversion of all of the three reaction mixture components was observed on Co–Mo catalysts prepared with the use of samples AMn containing ~1 mol % M<sub>x</sub>O<sub>y</sub> as supports, as compared with catalyst Co–Mo/A. An increase in the concentration of M<sub>x</sub>O<sub>y</sub> to 5 mol % was accompanied by a decrease in the rate constants of conversion of all of the three reaction mixture components, as compared with Co–Mo/Al<sub>2</sub>O<sub>3</sub>; moreover, the conversion of 4,6-DMDBT on Co–Mo/AL5 did not occur. Another behavior is characteristic of Co–Mo/AB5, for which k<sub>4,6</sub>-DMDBT is 3.3 h<sup>-1</sup>, which is greater than that for Co–Mo/A by a factor of about 1.4 (Table 7). It is believed that the above reaction mixture components are converted at different surface sites of a catalyst.

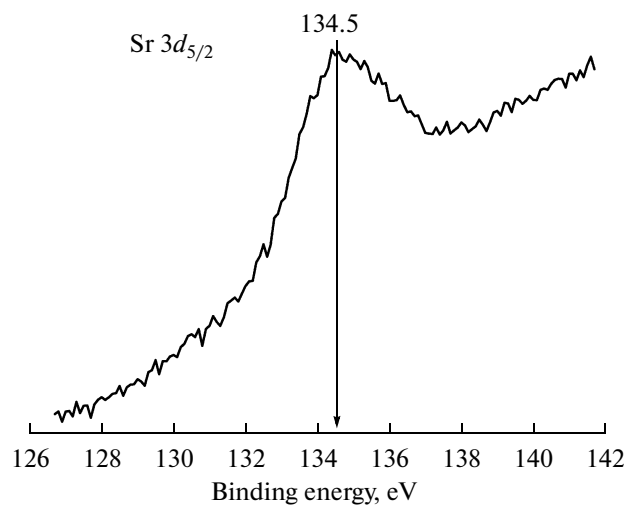


**Fig. 12.** The Sr 3d<sub>5/2</sub> XPS spectra of Co–Mo/AS1 samples.

A comparison of the rate constants of conversion of DBT and 4-MDBT on the test catalysts and the concentrations of LASs and BSs on the surfaces of corresponding supports AMn shows (Table 8) that the constants k<sub>DBT</sub> and k<sub>4</sub>-MDBT change in the same sequence: the greatest value was observed on the catalysts prepared with the use of supports AM1, where M is Sr or La. In this case, the lower the total surface concentration of LASs and BSs, the higher the rate constant of conversion with few exceptions (which are acceptable with consideration for current errors in the determination of rate constants and surface concentrations of acid and basic sites).

The above sequence changes for the rate constants of conversion of 4,6-DMDBT, namely, the highest

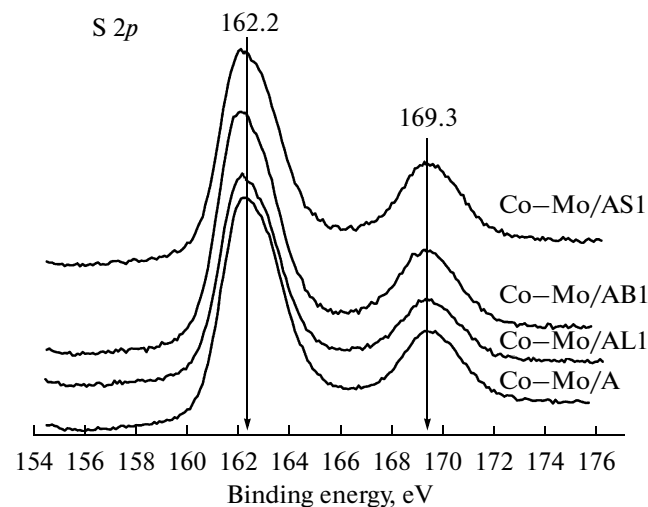


**Fig. 13.** The S 2p XPS spectra of Co–Mo/AM1 samples.

**Table 6.** Atomic concentrations of the elements on the surface of Co–Mo/AM1 samples according to XPS data

Sample	[Co]/[Mo]	[Mo]/[Al]	[Co]/[Al]	[O]/[Al]	[S]/[Al]	[Mo <sup>4+</sup> ]/[Mo <sub>total</sub> ]	[Mo <sup>4+</sup> ]/[Mo <sup>5+</sup> + Mo <sup>6+</sup> ]	[S <sub>d</sub> ]/[Mo <sup>4+</sup> ]	[S <sub>d</sub> ]/[S <sub>t</sub> ]
Co–Mo/A	0.39	0.109	0.042	1.98	0.28	0.73	1.75	2.98	2.50
Co–Mo/AS1	0.31	0.101	0.032	1.94	0.25	0.66	1.43	3.05	1.96
Co–Mo/AB1	0.35	0.098	0.035	2.01	0.23	0.69	1.28	3.14	2.13
Co–Mo/AL1	0.35	0.105	0.037	2.02	0.25	0.73	1.68	2.69	2.17

**Table 7.** Dependence of the pseudo-first-order rate constants of hydrodesulfurization on the nature of the catalyst for the reactions of DBT, 4-MDBT, and 4,6-DMDBT

Sample	<i>k</i> , h <sup>-1</sup>		
	DBT	4-MDBT	4,6-DMDBT
Co–Mo/A	13.3	5.9	2.4
Co–Mo/AS1	14.0	6.7	3.2
Co–Mo/AB1	13.0	6.0	2.8
Co–Mo/AL1	14.2	6.3	3.1
Co–Mo/AS5	7.3	3.9	2.0
Co–Mo/AB5	10.5	5.8	3.3
Co–Mo/AL5	4.3	1.6	0

rate of conversion was observed on Co–Mo/AB5 catalyst. In this case, the rate of conversion of this reaction mixture component depends on the concentration of weak LASs (absorption band at 2165–2175 cm<sup>-1</sup>), formed by coordinatively unsaturated M<sup>n+</sup> modifying

ions. We found that an optimum concentration of the above sites, which is 0.8–0.9 μmol/m<sup>2</sup> (AS1 and AB5), is necessary for reaching the greatest value of *k*<sub>4,6-DMDBT</sub>. A decrease and, especially, an increase in the concentration of weak LASs leads to a decrease in the values of

**Table 8.** Comparison between the rate constants of conversion of DBT, 4-MDBT, and 4,6-DMDBT on the test catalysts and the concentrations of LASs and BSs on the surface of corresponding supports

Sample	<i>k</i> <sub>DBT</sub> , h <sup>-1</sup>	<i>k</i> <sub>4-MDBT</sub> , h <sup>-1</sup>	ΣLASs, μmol/m <sup>2</sup>	ΣBSs, μmol/m <sup>2</sup>	<i>k</i> <sub>4,6-DMDBT</sub> , h <sup>-1</sup>	LASs (absorption band at 2165–2175 cm <sup>-1</sup> ), μmol/m <sup>2</sup>
Co–Mo/AL5	4.3	1.6	3.9	3.1	0	3.12
Co–Mo/AS5	7.3	3.9	2.8	2.6	2.0	1.61
Co–Mo/AB5	10.5	5.8	2.0	2.5	3.3	0.79
Co–Mo/AB1	13.0	6.0	1.7	2.4	2.8	0.40
Co–Mo/A	13.3	5.9	2.0	1.8	2.4	0
Co–Mo/AS1	14.0	6.7	2.6	2.1	3.2	0.91
Co–Mo/AL1	14.2	6.3	2.0	2.1	3.1	0.56

$k_{4,6\text{-DMDBT}}$ ; in particular, the conversion of 4,6-DMDBT does not occur at a concentration of these sites of  $3.12 \mu\text{mol}/\text{m}^2$  (AL5).

Consequently, for the effective transformation of DBT and 4-MDBT, the surface concentration of both LASs and BSs of the support should be minimal, whereas an optimum concentration of weak LASs (absorption band at  $2165\text{--}2175 \text{ cm}^{-1}$ ) is required for the conversion of 4,6-DMDBT. It is likely that the observed behaviors were caused by the fact that, at a minimum surface acidity and basicity, conditions that minimize the interaction of a Mo-containing component with the support are created to facilitate the more complete interaction between Co- and Mo-containing components and the formation of less dispersed particles. In turn, it is likely that the presence of a highly dispersed Mo-containing compound is required for the effective transformation of 4,6-DMDBT, which is ensured by its partial interaction with the coordinatively unsaturated  $\text{M}^{n+}$  ions of the support.

It was noted above that the rate constants of conversion  $k_{\text{DBT}}$  and  $k_{4\text{-MDBT}}$  increase in the order  $\text{Co-Mo/AB1} < \text{Co-Mo/A} < \text{Co-Mo/AS1} < \text{Co-Mo/AL1}$ , whereas  $k_{4,6\text{-DMDBT}}$  increase in the other order  $\text{Co-Mo/A} < \text{Co-Mo/AB1} < \text{Co-Mo/AL1} < \text{Co-Mo/AS1}$ . This means that the effective transformation of DBT and 4-MDBT was observed on Co-Mo/AL1, whose Co-Mo-S sulfide packets are characterized by the greatest sizes: along with single-layer packets with a diameter of 5–7 nm, five-layer packets to 20 nm in diameter were also present. Catalyst Co-Mo/AS1, which is the most active in the conversion of 4,6-DMDBT, contains the most dispersed Co-Mo-S sulfide packets, whose size can be as small as 2 nm. It is necessary to note that the  $[\text{Co}] : [\text{Mo}]$  surface atomic ratio and the fraction of molybdenum sulfide species decrease in the order  $\text{Co-Mo/A} > \text{Co-Mo/AB1} \approx \text{Co-Mo/AL1} > \text{Co-Mo/AS1}$ ; that is, the smallest degree of molybdenum reduction was observed in Co-Mo/AS1. However, for this catalyst, the degree of sulfidation, which is characterized by the  $[\text{S}_d] : [\text{Mo}^{4+}]$  ratio, is somewhat higher than that for other catalysts (Table 6), and it is the greatest for  $k_{4,6\text{-DMDBT}}$  (Table 7). The regularities obtained are consistent with the results of Andonova et al. [10], who observed a higher catalytic activity on catalyst Ni-Mo/Al-Ca, where the degree of molybdenum reduction to  $\text{Mo}^{4+}$  is lower and the degree of sulfidation (the  $\text{S} : \text{Mo}^{4+}$  ratio) is higher than those in a sample on the unmodified support. Thus, for the effective conversion of DBT, 4-MDBT, and 4,6-DMDBT, different degree of dispersion of Co-Mo-S sulfide packets and specific  $[\text{Co}] : [\text{Mo}]$  and  $[\text{S}] : [\text{Mo}^{4+}]$  surface atomic ratios are necessary.

Thus, the above study of Co-Mo catalysts supported on aluminum oxide modified with the cations of alkaline-earth and rare-earth elements (Sr, Ba, and

La) in 1 and 5 mol % concentrations showed that the nature and concentration of M is responsible for both the structural, textural, and acid-base properties of the support and the surface properties and degree of dispersion of Co-Mo-S sulfide packets and hence for activity in the conversion of DBT, 4-MDBT, and 4,6-DMDBT.

## ACKNOWLEDGMENTS

We are grateful to our colleagues from the Boreskov Institute of Catalysis, Siberian Branch, Russian Academy of Sciences: A.A. Budneva for her assistance in performing IR-spectroscopic experiments, D.A. Zyuzin for performing XRD analysis, and T.Ya. Efimenko for measuring the texture characteristics of the samples.

## REFERENCES

1. Song, C., *Catal. Today*, 2003, vol. 86, p. 211.
2. Babich, I.V. and Moulijn, J.A., *Fuel*, 2003, vol. 82, p. 607.
3. Topsøe, H., Clausen, B.S., and Massoth, F.E., *Hydrotreating Catalysis: Science and Technology*, Catalyst Science and Technology, vol. 11, Berlin: Springer, 1996.
4. Breysse, M., Afanasiev, P., Geantet, C., and Vrinat, M., *Catal. Today*, 2003, vol. 86, p. 5.
5. Pratt, K.C., Sanders, J.V., and Christov, V., *J. Catal.*, 1990, vol. 124, p. 416.
6. Iwamoto, R. and Grimblot, J., *J. Catal.*, 1997, vol. 17, p. 252.
7. Ramirez, J., Fuentes, S., Diaz, J.R., Fuentes, G., Vrinat, M., Breysse, M., and Lacroix, M., *Appl. Catal., A*, 1989, vol. 52, p. 211.
8. Okamoto, Y., *Catal. Today*, 1997, vol. 39, p. 45.
9. Rawat, K.S., Rana, M.S., and Murali Dhar, G., *Stud. Surf. Sci. Catal.*, 2001, vol. 135, p. 301.
10. Andonova, S., Vladov, Ch., Pawelec, B., Shtereva, I., Tyuliev, G., Damyanova, S., and Petrov, L., *Appl. Catal., A*, 2007, vol. 328, p. 201.
11. Caloch, B., Mohan S. Rana, and Ancheyta, J., *Catal. Today*, 2004, vol. 98, p. 91.
12. Guevara-Lara, A., Cruz-Pérez Alida, E., Contreras-Valdez, Z., Mogica-Betancourt, J., Alvarez-Hernandez, A., and Vrinat, M., *Catal. Today*, 2010, vol. 149, p. 288.
13. Klicpera, T. and Zdražil, M., *J. Catal.*, 2002, vol. 206, p. 314.
14. Zdražil, M., *Catal. Today*, 2003, vol. 86, p. 151.
15. Wu, L., Jiao, D., Wang, J., Chen, L., and Cao, F., *Catal. Commun.*, 2009, vol. 11, p. 302.
16. Paukshtis, E.A., *Infrakrasnaya spektroskopiya v geterogennom kislotno-osnovnom katalize* (Infrared Spectroscopy in Heterogeneous Acid-Base Catalysis), Novosibirsk: Nauka, 1992.
17. Scofield, J.H., *J. Electron Spectrosc. Relat. Phenom.*, 1976, vol. 8, p. 129.

18. Tanaka, K. and Ozaki, A., *J. Catal.*, 1967, vol. 8, p. 1.
19. Okamoto, Y., Nakano, H., Shimokawa, T., Imanaka, T., and Teranishi, S., *J. Catal.*, 1977, vol. 50, p. 447.
20. Brinen, J.S. and Armstrong, W.D., *J. Catal.*, 1978, vol. 54, p. 57.
21. De Jong, A.M., de Beer, V.H.J., van Veen, J.A.R., and Niemantsverdriet, J.W., *J. Phys. Chem.*, 1996, vol. 100, p. 17722.
22. Sanders, A.F.H., de Jong, A.M., de Beer, V.H.J., van Veen, J.A.R., and Niemantsverdriet, J.W., *Appl. Surf. Sci.*, 1999, vols. 144–145, p. 380.
23. Saih, Y. and Segawa, K., *Appl. Catal., A*, 2009, vol. 353, p. 258.
24. Rida, A., Benabbas, F., Bouremmad, F., Peña, M.A., and Martínez-Arias, A., *Catal. Commun.*, 2006, vol. 7, p. 963.
25. Bukhtiyarova, M.V., Ivanova, A.S., Plyasova, L.M., Litvak, G.S., Rogov, V.A., Kaichev, V.V., Slavinskaya, E.M., Kuznetsov, P.A., and Polukhina, I.A., *Appl. Catal., A*, 2009, vol. 357, p. 193.
26. Rousseau, S., Loridant, S., Delichere, P., Boreave, A., Deloume, J.P., and Vernoux, P., *Appl. Catal., B*, 2009, vol. 88, p. 438.
27. Sosulinikov, M.I. and Teterin, Yu.A., *J. Electron Spectrosc. Relat. Phenom.*, 1992, vol. 59, p. 111.
28. Dupin, J.-C., Gonbeau, D., Vinatier, P., and Levasseur, A., *Phys. Chem. Chem. Phys.*, 2000, vol. 2, p. 1319.
29. Van der Heide, P.A.W., *J. Electron Spectrosc. Relat. Phenom.*, 2006, vol. 151, p. 79.
30. Hueso, J.L., Caballero, A., Ocaña, M., and González-Elipe, A.R., *J. Catal.*, 2008, vol. 257, p. 334.
31. Zhuang, S.-X., Yamazaki, M., Omata, K., Takahashi, Y., and Yamada, M., *Appl. Catal., B*, 2001, vol. 31, p. 133.
32. Rodríguez-Castellón, E., Jiménez-López, A., and Eliche-Quesada, D., *Fuel*, 2008, vol. 87, p. 1195.